1 Astrometry is a foundation of astronomy

The determination of the motion of celestial bodies through repeated measurements of their position using astrometric techniques constitutes the foundation of our present understanding of the Universe. For consistency in time and space, and hence comparisons for different celestial bodies, such determinations must be established in well-defined coordinate (or reference) systems. In practice, these celestial systems are not defined directly but only implicitly through recording electro-magnetic emission of celestial bodies taken as fiducial at ground stations. Tables with precise positions, distances, and proper motions of fiducial bodies are called catalogues and the outcome of observing programs that often take decades to accomplish.

Astrometric catalogues are foundation of astronomy: a position of the celestial body uniquely discriminates it from other bodies. Measurement of motion of celestial bodies allows us to study forces that caused their motion.

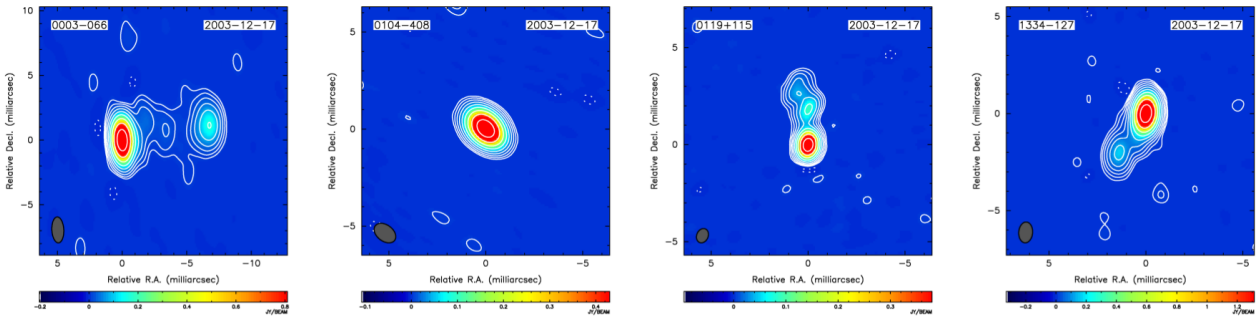

Figure 1: A sample of VLBI maps from the Bordeaux VLBI Image Database (Collioud & Charlot, 2014) showing the predominantly core-jet structure of the AGNs on milliarcsecond scales.

Coordinates of celestial bodies can be determined together with positions of observing stations and rotation parameters of the terrestrial coordinate system with respect to the celestial system (so-called Earth orientation parameters). Positions determined in such a way are called absolute positions. Absolute astrometry programs have to be scheduled in a special way, and their analysis is highly sophisticated since a number of subtle effects, such as crustal deformation caused by variations in the atmospheric pressure (see f.e., Petrov & Boy, 2004), need to be accounted for. An absolute astrometric catalogue has three free parameters that determine the absolute orientation of the coordinate system that are not measurable in principle and are established by a convention. But other than these three free parameters, absolute position of a given celestial body do not dependent on position of another bodies. In contrast, differential astrometry observations are much more simple. They determine a displacement of a target body with respect to a reference body that in radioastronomy is often called a calibrator. Although a position of a target body cannot be determined more precisely than a position of a calibrator, the difference in positions is usually measured more precisely, since many systematic errors are approximately scaled as the target/calibrator separation expressed in radians. This is sufficient for a number of applications, for instance, for determination of a parallax and/or proper motion of a Galactic object, such as a star or a maser. However, differential astrometry is possible only if the absolute astrometry catalogue is available and a calibrator position is known as being stable. It is a challenge to derive an absolute astrometry catalogue of stars, since the great majority of stars have non-negligible proper motions. Errors in proper motion will affect star positions stronger and stronger for the epochs that are further and further away from the middle epoch of observations used for deriving position of a star and its proper motion. Therefore, astronomers have a strong demand on observing "non-movable" objects for the needs of absolute astrometry. Selection of extragalactic objects that are supposed to a have negligible tangential motion just because they are so far away is

a natural choice. But observing galaxies for astrometry using an optical instrument is problematic because galaxies are diffuse objects. It is difficult to determine positions of diffuse object precisely.

1.1 VLBI absolute astrometry

VLBI is sensitive to emission at milliarcsecond scales. Active galaxy nuclei powered by the accretion of matter to supermassive black-hole turned out ideal objects for precise radio astrometry. These objects are very remote — they are located at gigaparsec distances, very bright — with brightness temperature 10^7–10^{13} K, have very compact cores with sizes less than one milliarcsecond, and emit a broadband continuum signal. The technique of VLBI absolute astrometry was established in 1970s. The first VLBI absolute astrometry catalogue (Cohen & Shaffer, 1971) had 35 objects and provided arcsecond accuracy. Since then, owing to dedicated observational programs for almost 50 years (Ma et al., 1998; Beasley et al., 2002; Fomalont et al., 2003; Petrov et al., 2005, 2006, 2008, 2011a,b, 2019b; Petrov, 2012, 2011, 2013, 2016; Immer et al., 2011; Petrov & Taylor, 2011; Shu et al., 2016; Kovalev et al., 2007; Gordon et al., 2016), the number of sources with precise positions grew by three order of magnitude.

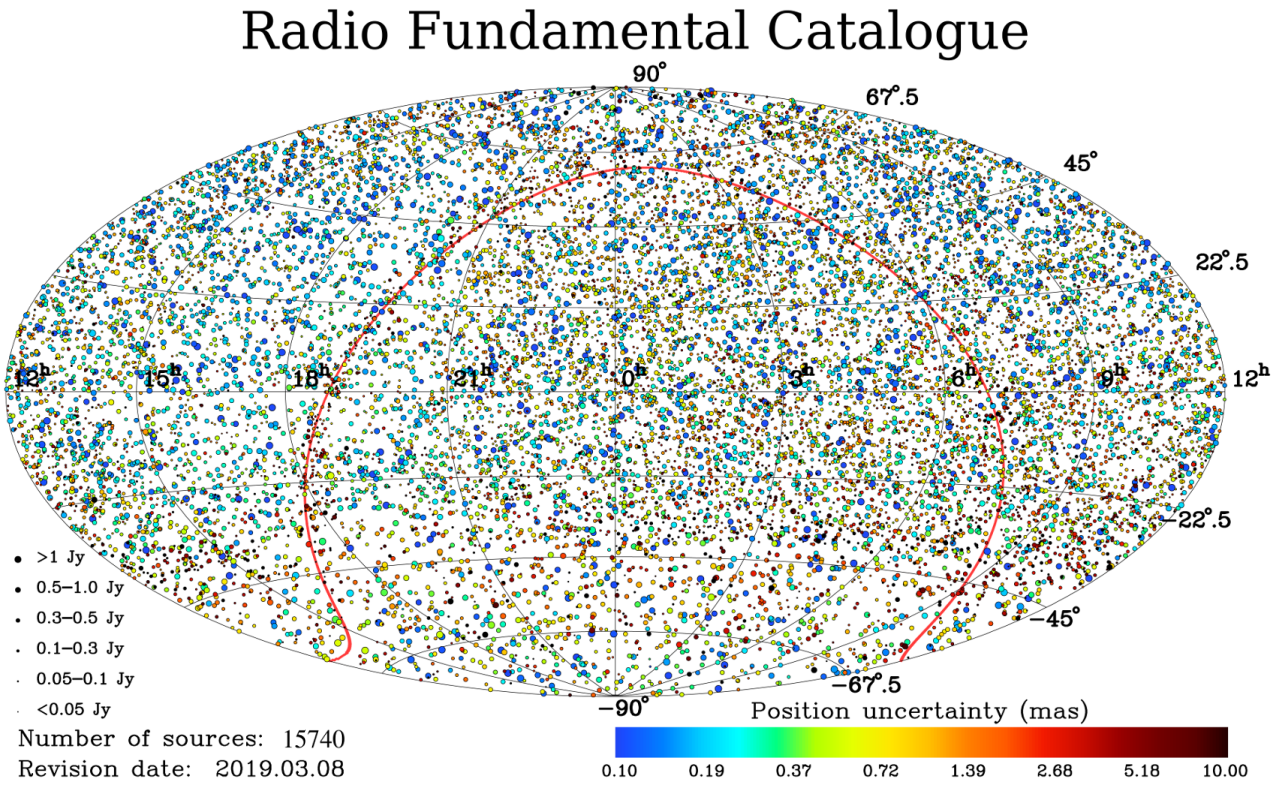

Figure 2: The distribution of the sources which positions were determined from processing the data collected under VLBI absolute astrometry programs.

The most comprehensive VLBI position catalogue to date is the Radio Fundamental Catalogue or RFC available at http://astrogeo.org/rfc (Petrov and Kovalev, 2019 in preparation). By 2019, the RFC comprises positions for 15,740 extragalactic objects, and since the observing program is still going, the number of sources to be included in the next release of the catalogue will be growing. FITS images at 2.3, 5.0, 8.4, 15, and/or 24 GHz of over 14,000 RFC sources are publicly available at http://astrogeo.org/vlbi_images. The median position uncertainty is 0.8 mas. The RFC has the median flux density 100 mJy at 8 GHz. It is complete at 150 mJy at 8 GHz at the 95% level. A subset of the sources that were observed more intensively at 2.3 and 8 GHz simultaneously, as

well as at 24 and 32 GHz, and therefore, have a better position accuracy than on average, forms the catalogue known as the third realization of the International Celestial Reference Frame, ICRF3 (Charlot et al. in preparation). The ICRF3 has median positional errors of the order of 0.1 mas in right ascension and 0.2 mas in declination with a claimed noise floor of 0.03 mas in the individual coordinate.

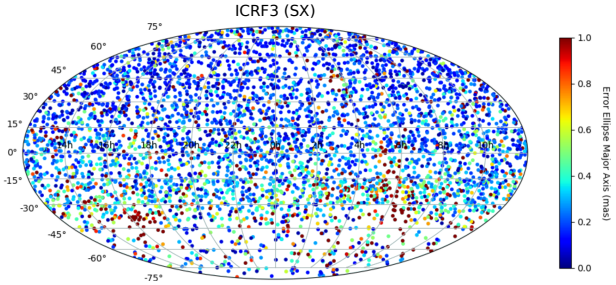

Figure 3: A subset of 29% RFC sources that were intensively observed in follow-up dual-band 2.3/8.4 GHz VLBI campaigns as well as at 24 and 32 GHz. Positions of these sources are presented in the ICRF3 catalogue.

2 Absolute astrometry as a community service

Absolute astrometry provides a grid of sources with precisely known positions. Such a grid is in high demand for a number of applications, many of them are not feasible without absolute astrometry. Therefore, an activity for densification of the grid, and improvement of their positions, determining their other properties, such as images, spectral index, positional stability is an important service for the astronomical community as a whole.

2.1 Differential astrometry

Observational technique that points radiotelescopes first to the target with known position then to slews to a target and back allows determine very precisely an offset of a target with respect to the calibrators. Such observations are also called nodding. The contribution of systematic errors, notably the atmosphere, dilutes at the extent proportionally to the target/calibrator separation. Accuracies 0.03–0.05 mas are achievable for carefully scheduled observations with target/calibrator separations < 2–$3°$. Differential astrometry is capable to density absolute astrometry catalogues, see for instance (Deller & Middelberg, 2014). Reid & Honma (2014) provide an overview of the application of differential astrometry for measurement of parallaxes and proper motions of masers in the star forming regions (Xu et al., 2013; Reid et al., 2014), evolved asymptotic giant branch (AGB) stars (Kurayama et al., 2005), and X-ray binaries (Reid et al., 2011). Differential astrometry was also used for pulsars parallax determination (Deller et al., 2019). Measurements of parallaxes at kiloparsec distances allow us to understand the spiral structure of the Milky Way probing the objects that are either too obscured by the dust in the Galactic plane to be visible in the optical range, or have very faint optical emission below the detection limit of optical telescopes as pulsars. Knowledge of distance is critical for quantitative measures of cloud and young stellar object sizes, masses, luminosities, and ages.

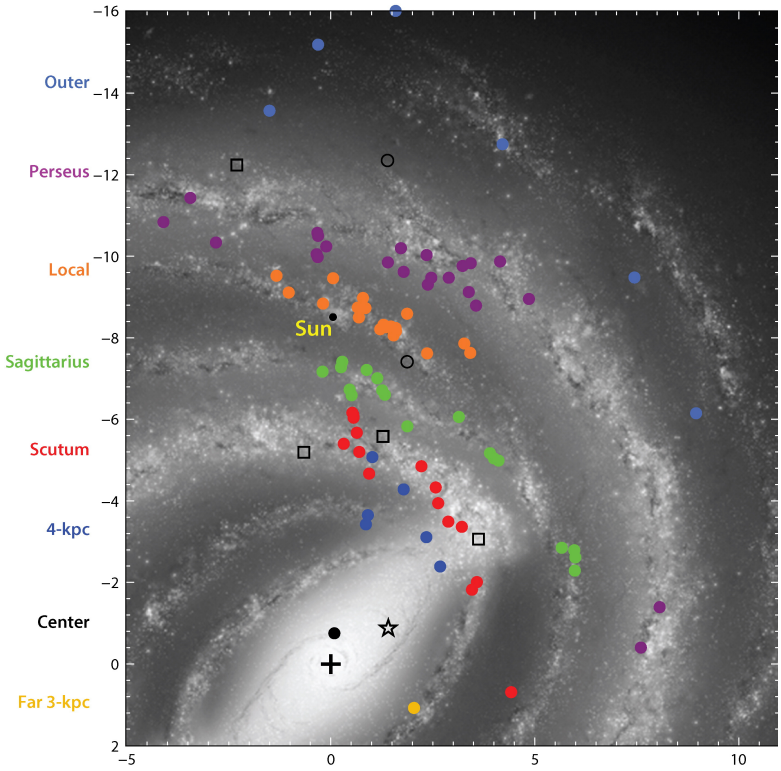

Reid MJ, Honma M. 2014.
Annu. Rev. Astron. Astrophys. 52:339–72

Figure 4: Plan view of the Milky Way. The background is an artist conception, guided by VLBI astrometry and Spitzer Space Telescope photometry (R. Hurt: IPAC). Colored dots are the locations of newly formed OB-type stars determined from trigonometric parallaxes using associated maser emission. The parallaxes were determined with VLBI. Reproduced from Reid & Honma (2014)

2.2 The use of the reference calibrator sources for observing weak targets

Nodding observations have another very important application. Atmospheric phase fluctuations set the limit of how long a source can be observed. Integration time determines the faintest source that can be detected. However, the differences in phases of close pair of objects have smaller fluctuations than the total phases. Therefore, using nodding observations, one can extend integration time and lower the limit of the faintest objects detected. The presence of a relatively strong calibrator with a known position in the vicinity of a target is a prerequisite for observations of faint objects. Nowadays, more than half of observations are made in the phase reference mode. The absolute astrometry catalogue provide the list of such calibrators and thus, make observations of weak objects feasible.

2.3 The use of astrometry for Earth sciences

Precise measurements of group delays allows us to determine the projection of the baseline vector to the source direction with a millimeter level precision. Positions of the radiotelescope reference points and parameters of the Earth rotation can be determined from analysis of observations of sufficiently large list of radio sources with an accuracy that corresponds to a millimeter level and is limited mainly by our ability to model path delay in the neutral atmosphere. Since the AGNs observed with VLBI for Earth orientation parameter (EOP) determination have redshifts 1–3, the EOPs measured that way are determined with respect to a truly non-rotating coordinate system. In contrast, the

EOP determined using satellite techniques, such as GNSS, SLR, and DORIS suffer from systematic errors associated with a secular change of orbital elements that are difficult to model and account for. In particular, uncertainties in modeling ascending nodes of GNSS orbits for radiation pressure and drag in the upper atmosphere are especially large, making determination of the EOP that describes axial rotation (UT1–UTC) and precession-nutation parameters from these observation too biased to be useful. VLBI is the only technique that allows unbiased determination of UT1–UTC and nutation angles (Fig. 5).

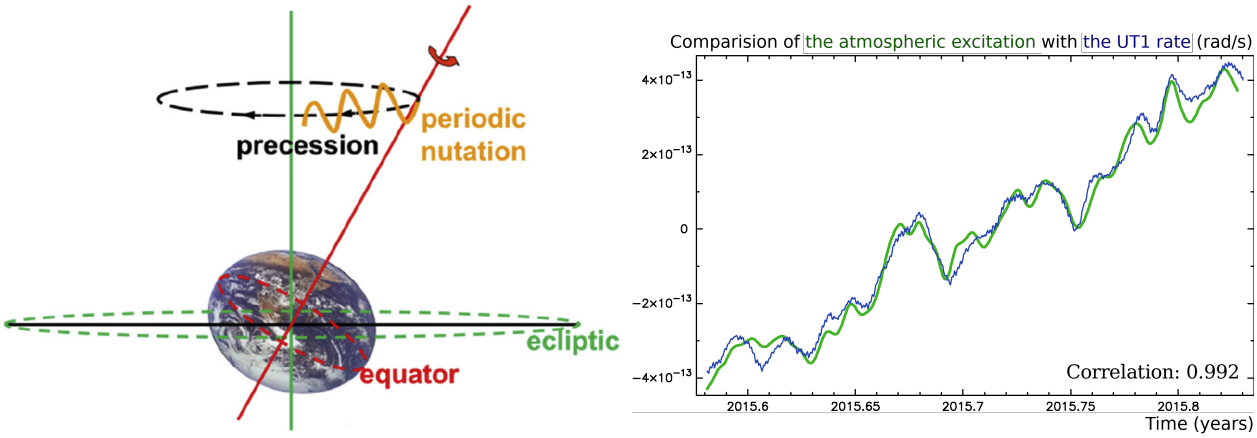

Figure 5: *Left:* Representation of precession and nutation of the Earth (Fig. 1 in Dehant et al., 2017). *Right:* Comparison of the atmospheric excitation computed using NASA numerical weather model GEOS-FPIT and the axial rotation rate (UT1 rate) determined using VLBI observations.

Variations in UT1–UTC in a large extent and in nutation up to some extent are driven by exchange of the angular momentum between the atmosphere, hydrosphere, and crust. Since the total angular momentum of the Earth is conserved, an increase in the angular momentum of the atmosphere must be compensated by a decrease in the angular momentum of the crust. Atmospheric circulation is at a large extent unpredictable. Therefore, the EOP should be observed continuously. Although in the future accuracy of numerical atmospheric weather model may reach that level that variations in the Earth rotation can be derived directly using from these models, the current accuracy of numerical weather models is insufficient to derive the EOP with the accuracy comparable with accuracy of their estimates from VLBI observations.

The observed nutation amplitude deviated from the amplitudes of the rigid Earth at a level of 500–700 σ. Therefore, studying nutation motion allows us to learn about elastic and inelastic properties of the Earth's interior (Mathews et al., 2002; Rosat et al., 2017). Inversion of the precession-nutation complex amplitudes allows us to compute very precisely dynamic flattening of the whole Earth's and the liquid core, coupling parameters at the core-mantle boundary, compliance parameters that are integrals over a function that include distribution of Earth's density and elasticity parameters with depth.

Key challenges in this area is explanation of the observed nutation amplitudes (Dehant & Mathews, 2015) that include 1) constraining models of mantle inelasticity; 2) constraining models of coupling the core-mantle boundary; 3) the detection of the contribution of the Earth's solid inner core, 4) a closure of the error budget between the modeled and observed nutations excited by the atmosphere, 5) understanding of the origin of the excitation and dissipation of the free core nutation. The latter also requires progress in global circulation models and in the theory of the Earth's rotation.

3 Science with absolute astrometry

In addition to supporting various fields of astronomy, absolute astrometry enables interesting science per see.

3.1 VLBI/Gaia offsets

On September 16 2016, the Gaia data release 1 (Lindegren et al., 2016) ushered a revolution in optical astrometry. Approximately 60% of RFC sources have a counterpart with Gaia, other sources are too weak for Gaia detection. A quick analysis by Mignard et al. (2016) found that in general, the differences between common AGNs in VLBI and Gaia DR1 catalogues are close to their uncertainties, however there exists a population of sources with statistically significant position differences. Extensive analysis of Petrov & Kovalev (2017a) showed that such factors as the failures in quality control in both VLBI and Gaia, blended nearby stars, or bright host galaxies can account at maximum for 1/3 of that population. This analysis, as well as works of Mignard et al. (2016); Makarov et al. (2017); Frouard et al. (2018); Liu et al. (2018a,b,c), used arc lengths of VLBI/Gaia differences. Further investigation of the distribution of the position angles with respect to the jet directions determined from analysis of VLBI images of matched sources revealed a strong anisotropy (Kovalev et al., 2017): the offsets have a preferable direction along the jet, and at a smaller extent in the direction opposite to the jet (See Fig. 6). Kovalev et al. (2017) suggested interpretation of this anisotropy as the presence of optical jets at scales finer than the Gaia point spread function (PSF), i.e., 100–300 mas. It was shown in Petrov & Kovalev (2017b) that because the response to an extended structure of a power detector used by Gaia and an interferometer that records voltage is fundamentally different, the presence of co-spacial optical structure will cause observed offset. The physical meaning of a VLBI/Gaia offset is a displacement of the optical centroid with respect to the jet base. Therefore, measuring this offset, we can make an inference about the property of optical jets that are too short to be detected directly with optical telescopes, including the HST. A new observable, VLBI/Gaia offset, augments the parameters space for AGN physics.

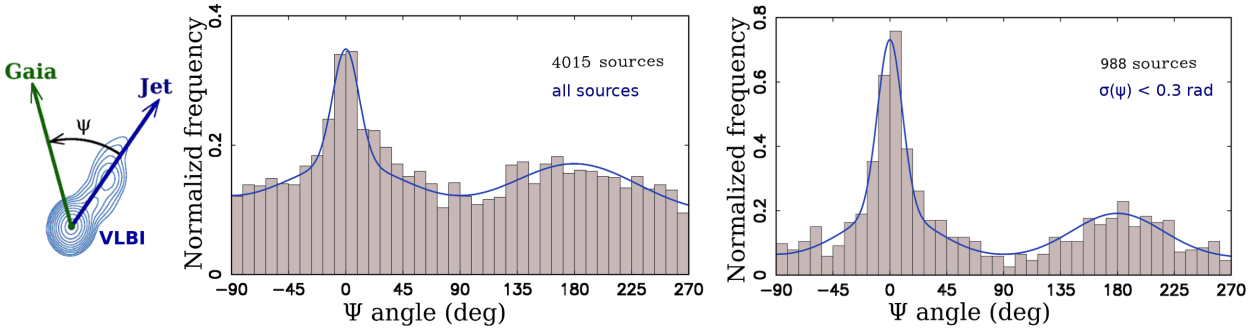

Figure 6: The distribution of VLBI/Gaia position offset angles with respect to jet directions. *Center:* the whole sample. *Right:* a subset of sources with position angles determined with 1-σ errors smaller than 0.3 rad. Reproduced from Petrov et al. (2019a).

The power of this approach was demonstrated in Plavin et al. (2019b). Analysis of optical color shows that AGNs of different class have different preferred direction of the VLBI/Gaia offsets. Just a direction of VLBI/Gaia offsets allows us to discriminate synchrotron dominated, redder sources that have Gaia positions shifted with respect to VLBI positions along the jet, and accretion disk dominated, bluer objects that have Gaia positions shifted in the opposite direction.

It was predicted in Petrov & Kovalev (2017b) that Gaia positions of AGNs will have a jitter because the variability will affect position of the centroid and that a combined analysis of Gaia light

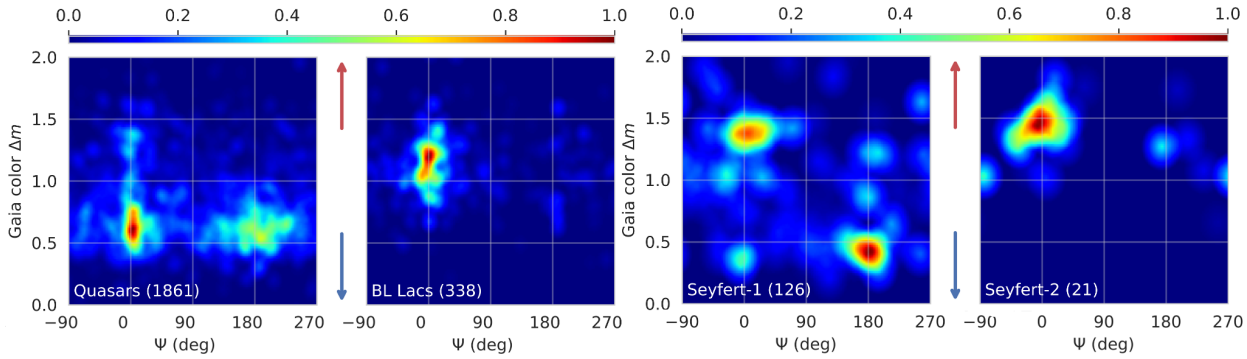

Figure 7: The pairwise distribution of the angle ψ of the VLBI/Gaia offset direction wrt jet direction with optical color index shown separately for different classes of AGNs. Reproduced from Plavin et al. (2019b).

curves and time series of VLBI/Gaia offsets will probably allow recovery of properties of the optical core-jet morphology: the position of the jet centroid, its flux density and, in some simple cases, kinematics. Analysis of these series has the potential to locate the region where the optical flare occurs: the core, accretion disc or jet features.

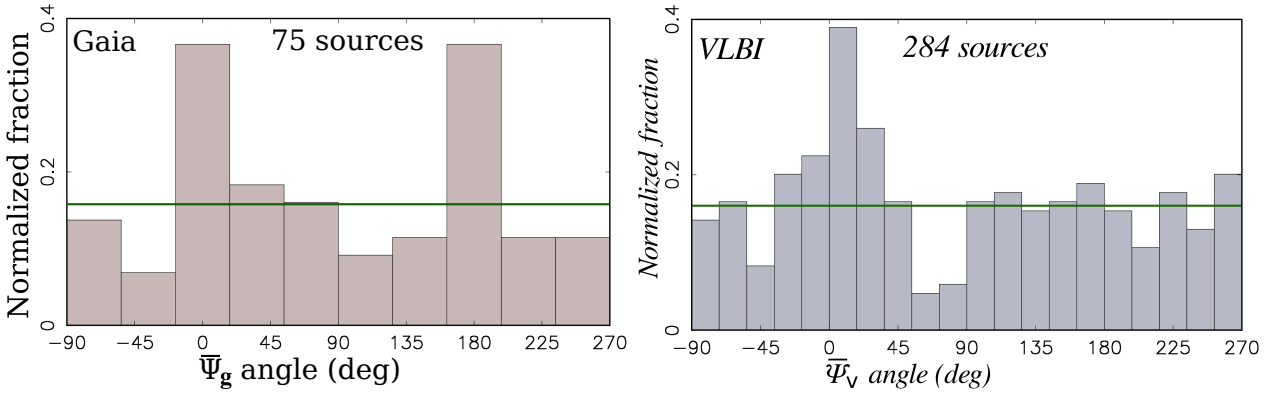

Figure 8: The histograms of significant AGNs proper motion position angles with respect to jet directions among matched sources. *Left:* the Gaia DR2 proper motions with magnitudes $> 3\sigma$ in both proper motions and position offsets. The median magnitude is 1.15 mas/yr. *Right:* the VLBI proper motions from a global solution The median magnitude is 0.02 mas/yr. Reproduced from Petrov et al. (2019a).

The prediction of Gaia jitter has been confirmed indirectly from analysis of 9083 offsets between VLBI positions and Gaia data release 2 by Petrov et al. (2019a). The AGN proper motions reported by Gaia show a strong preference to the direction along or opposite the jet (see left plot in Fig. 8). VLBI technique also detects proper motion of AGNs, and the proper motion directions also have a preference towards jet direction (see right plot in Fig. 8), but the median magnitude of AGN proper motion determined with VLBI is a factor of 52 less. That gives us strong evidence that the Gaia AGN proper motion of the centroid is caused by optical flux variations, not by a transverse bulk motion. An instability of optic AGN position due to flux variability and the presence of milli-arcsecond structure is a new phenomenon that needs to be studied and understood. We now know that starting from tens nrad level (1–5 mas) VLBI and Gaia positions disagree and new observations will not reconcile them, but will measure this variable offsets more and more precisely. That brings a number of important consequences. Since VLBI positions related to the brightest AGN feature divert from Gaia positions

related to the centroid position, we cannot borrow Gaia positions for the use in radio applications that require the highest accuracy, such as space navigation and space geodesy, is needed and we need maintain the radio coordinate system.

Since VLBI/Gaia position offsets provide a unique capability to have an insight to optical jets at distances 1–100 mas, not accessible to any other instrument, precise measurement of these offset will remain a priority in the future. For the majority of 9083 common AGNs with known VLBI/Gaia offsets, accuracy of their VLBI position is worse than accuracy of Gaia position. Therefore, more observing program targeted in improvement VLBI positions of these sources are anticipated in the future. The key scientific questions are 1) explanation of the Gaia offsets wrt radio core in the direction opposite to the jet; 2) quantitative characterization of optical jets; 3) pinpointing the areas in the AGNs where flare happen; 4) investigation of the dichotomy of the sources with thermal accretion-disk dominated and non-thermal synchrotron dominated optical emission. Solving these problem will require more observations for precise astrometry and high image fidelity or a sample up to 10,000 objects.

3.2 Core-shift

In VLBI images of relativistic AGN jets, the 'core' is typically identified with the most compact component closest to the jet base. It is usually interpreted as the region with optical depth ≈ 1, which position depends on observing frequency (Blandford & Königl, 1979; Kovalev et al., 2008). Observations confirm (see part of Fig. 9) that the core is located farther from the jet base and has larger apparent size at lower frequencies (e.g., Sokolovsky et al., 2011).

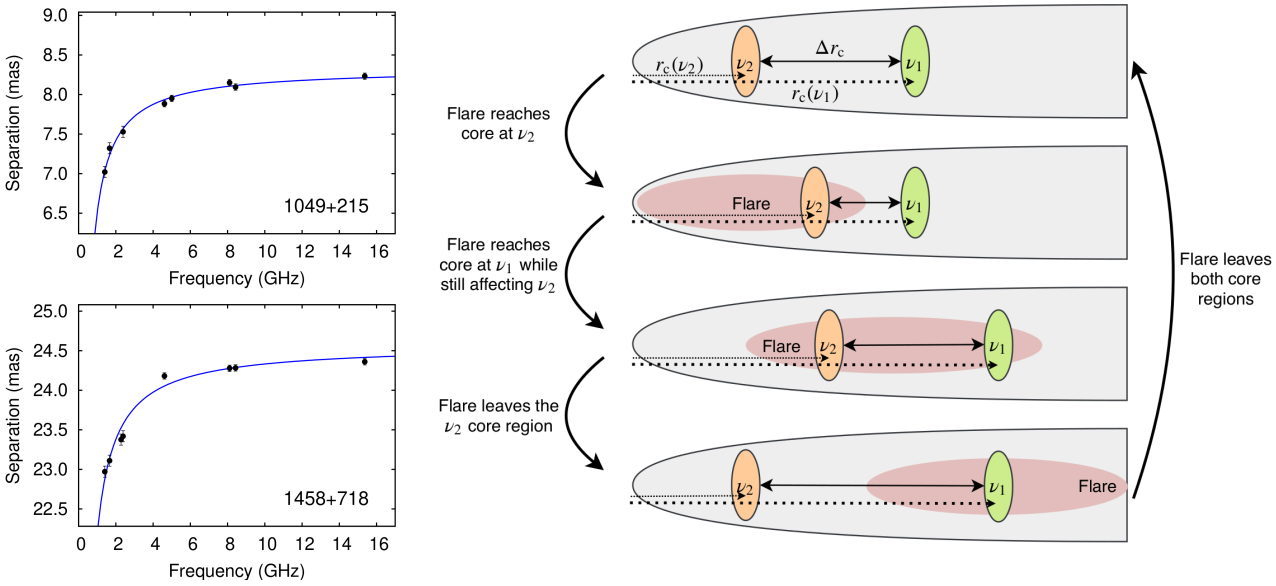

Figure 9: *Left:* Separation of the core from a reference optically-thin jet component as a function of frequency from analysis of VLBI observations. The curve represents the best-fit function $r_c(f) = a + b/f$. Reproduced from Sokolovsky et al. (Fig. 3 2011). *Right:* Propagation of a flare along the jet, shown schematically. Reproduced from Plavin et al. (2019a).

The dependence of the core-shift on frequency f for the most of the sources is close f^{-1} (Sokolovsky et al., 2011; Pushkarev et al., 2012). That corresponds to magnetic field decreasing proportionally to the distance from jet apex, and particle density decreasing proportionally to its square. As can be easily shown, (f.e., Porcas, 2009) in that case the contribution of the core-shift to group delays and phase delays used for astrometry data analysis is not distinguishable from the

contribution of the ionosphere. It vanishes when the ionosphere-free combination of dual-band observables is used for data analysis as it is done for the majority of absolute astrometry programs. Kutkin et al. (2019) have demonstrated that core-shift and total flux density time delay measurements measurements enable us to probe the kinematics of the extragalactic jets.

Plavin et al. (2019a) have shown that the core positions are variable in time, and this variability is closely related to AGN flaring activity. Under some broad assumptions, variability of the core flux density would be primarily caused by temporal variations of one of three basic properties of the relativistic plasma flowing through the core region: particle density, magnetic field, or the bulk Doppler factor. Combined analysis of the core-shift time series and light curves allows us to derive relativistic particle density and magnetic field variability.

Analysis in Plavin et al. (2019a) have also shown that during flares the condition of equipartition is expected to be violated since the particle density rapidly changed. The dependence of the core position on frequency is expected to change and dual-band observables will be affected by the core-shift. Indeed, those results imply that strong flares disrupt any regular frequency dependence of core positions, hence also affecting astrometric inferences. It should be noted, that data reduction for the extended source structure in astrometric solutions does not get rid of the core shift contribution. This effect is present even for point-like objects with no extended radio jets.

Therefore, the core-shift variability needs to be monitored for highly accurate astrometric programs. From one hand, variations in core-shift provide important information about the process in the vicinity of the core, and in particular help to understand the mechanisms of jet acceleration (Kutkin et al., 2019). From the other hand, measurements of core-shift variations are needed for fine reduction of astrometric data.

3.3 Search for inspiraling, binary, and recoiling black holes in nearby galaxies

As the term "active galactic nuclei" suggests, supermassive black holes were originally assumed to be at rest in the nuclei of their host galaxies because dynamical friction against the surrounding stars and gas will eventually make an offset SMBH in an isolated galaxy sink to the bottom of the host galaxy gravitational potential. However, the stellar bulges of nearly all galaxies contain SMBHs, so hierarchical merging of galaxies should frequently produce massive stellar bulges containing two or more SMBHs temporarily offset in position and velocity. Following a galaxy merger, a pair of inspiraling SMBHs may spend $\sim 10^8$ yr at separations ~ 1 kpc (Begelman et al., 1980) before forming a tight SMBH binary with ~ 1 pc separation, at which point the binary looks like a point mass to most of the stars causing dynamical friction and the contraction may stall. Such sources can be found in dedicated surveys by comparing their VLBI position that corresponds to the position of the black hole and optical in IR position that corresponds to the center of mass of stellar population. Fig. 10 illustrates a finding of an AGN at $2.8''$ of the brightest cluster galaxy and a dual AGN at $1.8''$ separation with two jet-powered compact radio sources. SMBH merger trees are a key component of the theoretical treatment of galaxy-SMBH co-evolution, but observations have yet to test this treatment in a serious way beyond these SMBH correlations. VLBI surveys are indispensable for identifying such objects that will allow us to build statistics of these unusual sources and will help us to constrain the theories of galaxy evolution.

3.4 VLBI astrometry of pulsars

Neutron stars can be seen from the radio to gamma-rays and provide unique laboratories to study matter and gravity in extreme environments that cannot be reproduced on Earth. Moreover, the extraordinarily regular and predictable rotation of some neutron stars permits their use as precise clocks, enabling probes of the interstellar medium, the motion of the Earth and the solar system, and exquisite tests of gravity. However, the science which is possible with these versatile objects is often

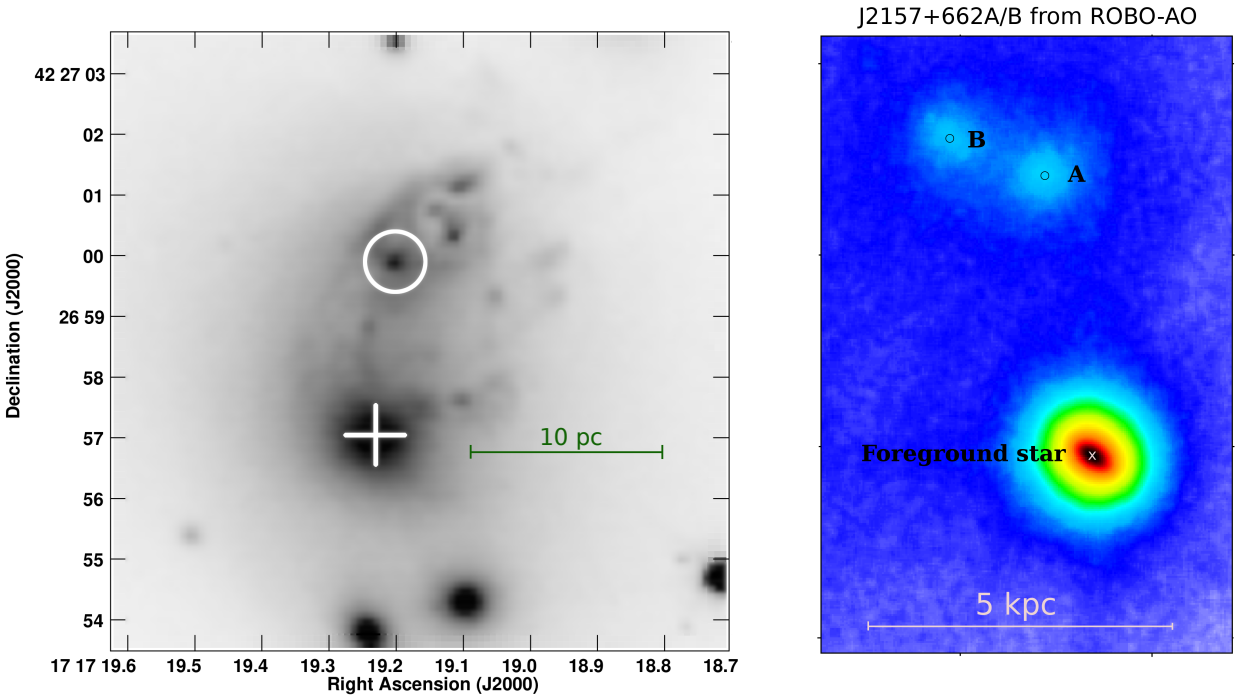

Figure 10: *Left:* HST F606W image of ZwCl 8183 that reveals the core of the brightest cluster galaxy, the radio galaxy, several cluster galaxies, and extended interaction debris. The HST position of the brightest cluster galaxy galaxy core is marked by the white +, and our new optical identification of B3 1715+425 is enclosed by a white circle centered on its HST position. Reproduced from Condon et al. (2017). *Right:* Robo-AO image of the dual AGN J2157+662A/B with two jet-powered compact radio sources separated at 1.8″ (Petrov & Duev, in preparation).

limited by the poorly known distance to the neutron star(s) in question. VLBI provides a unique capability to measure their parallaxes using differential astrometry with accuracy down to 0.03 mas, proper motions with accuracy 0.02 mas/yr, and find orbital motion of the pulsar in binary system with semi-major axes as small as 0.08 mas (Deller et al., 2013). The availability of parallax estimates of pulsars with accuracies better 1% (Deller et al., 2019) for a large samples have revolutionized the field.

The dynamical coordinate system used for pulsar timing can have an arbitrary orientation with respect to this kinematic coordinate system, which is described with three rotation angles. The orientation of the dynamical coordinate system used for pulsar timing is determined by the orientation of the Earth's orbit, and any residual error in this orientation can only be identified and corrected by observations of common objects. Comparing position of millisecond pulsars from pulsar timing with their positions from VLBI allows to determine orientation of the ecliptic plane with respect to remote AGNs at an accuracy down to tens of microarcsecond. The scatter of the differences between VLBI and pulsar timing provide an important independent checks of pulsar timing accuracy that is important for evaluation of detectability of gravitational wave background that the pulsar timing array is expected to be sensitive.

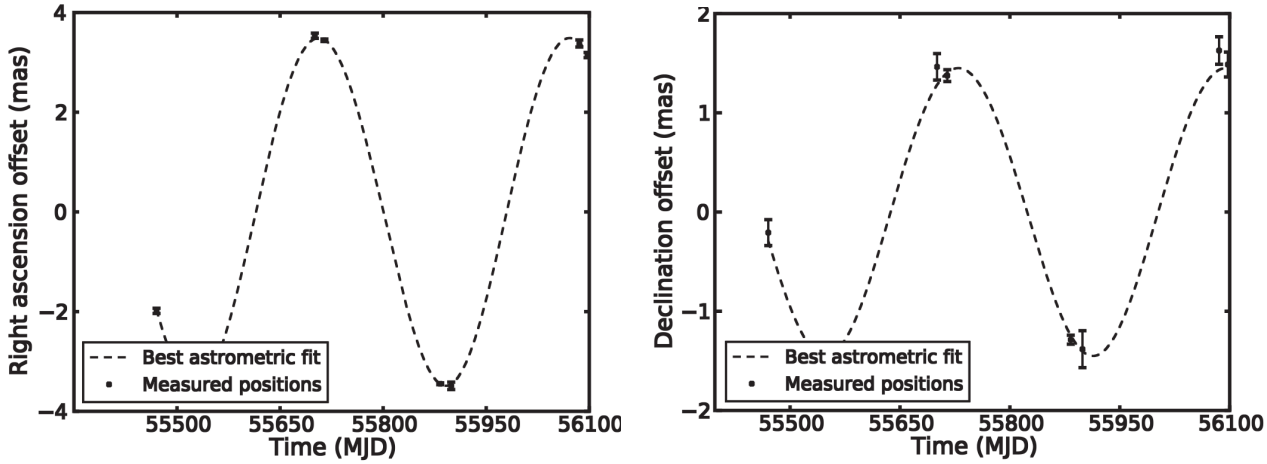

Figure 11: Astrometric fit to the positions obtained for PSR J2222–0137, highlighting the parallax signature. Reproduced from Deller et al. (2013).

3.5 Galactic aberration

Acceleration of the solar system in the gravitational field of our Galaxy results in an apparent secular motion of every objects with the magnitude $\mu = \frac{a}{c} \sin \zeta$, were a is the magnitude of the acceleration and ζ is the angle between the direction toward the Galactic center and that to the AGN (Kovalevsky, 2003; Kopeikin & Makarov, 2006). This effect, called galactic aberration, reaches 4–5μas/yr and is quite observable (Titov et al., 2011). The vector of the acceleration of the Solar system barycenter with respect to the remote AGN can be estimated. Analysis of the stellar dynamics and direct measurements distance to the Galactic center (Reid et al., 2009) provide an independent estimate of the galactic acceleration. Comparison of these estimates provides an important test of out understanding of stellar dynamics. Continued observing and accumulation of data in the future will further improve the estimate of the acceleration vector from VLBI and determine whether the motion of the Solar System is purely towards the Galactic center or whether it has an off-plane component. Systematic errors in VLBI source positions caused by the contribution of source structure and its changes affects the estimate of the acceleration vector and the magnitude of this contribution is poorly understood. Applying sources structure contribution in the data analysis and in depth evaluation of the uncertainties of this contribution is a key for providing a robust estimate of the acceleration vector and its uncertainty.

3.6 Cosmology and gravitational waves

Stochastic gravitational waves deflect light rays in a quadrupolar pattern. The gravitational waves that will produce extragalactic proper motions lie in the frequency range 10^{-18} Hz $< f < 10^{-8}$ Hz, which overlaps CMB polarization regimes and the pulsar timing, but uniquely covers about seven orders of magnitude of frequency space between the two methods (Gwinn et al., 1997; Darling et al., 2018b,a). Measuring or constraining the proper motion quadrupole power can therefore detect or place limits on primordial gravitational waves in a unique portion of the gravitational wave spectrum. Measurement of precise proper motions of supermassive black hole residing the AGNs enables us to assess another cosmological parameters: baryonic acoustic oscillations — the observed overdensity of galaxies on the scale of 150 Mpc in co-moving coordinates. At z=0.5, the propose motions associated with baryonic acoustic oscillations are of order of 1 μas/yr (Darling et al., 2018a). Anisotropic Universe expansion will cause a pattern of proper motions $\Delta H/H_0$ 15 μas/yr (Darling et al., 2018a). A detection of a signal 1 μas/yr with that patter will correspond to variations in the expansion rate

at a level of 7%.

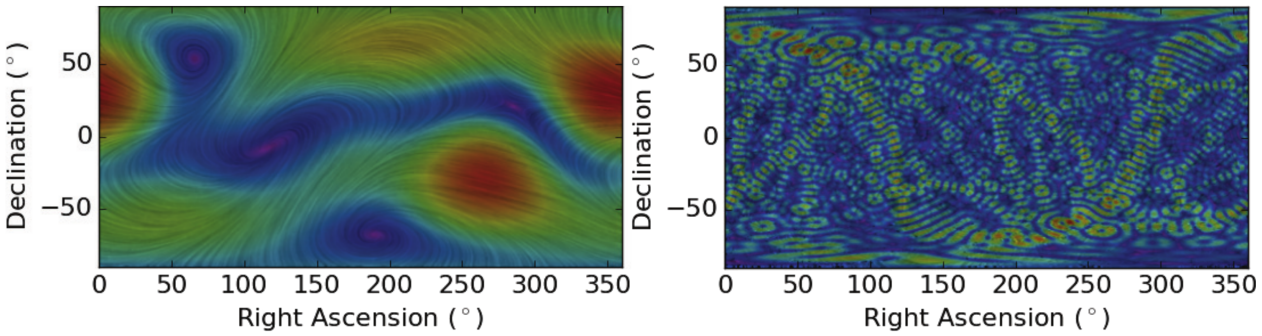

Figure 12: All-sky stream plots. Streamlines indicate the vector field direction, and the colors indicate the vector amplitude, from violet (zero) to red (maximum). *Left:* Randomly generated gravitational wave stream plot. *Right:* Randomly generated baryon acoustic oscillation streamlines. Reproduced from Darling et al. (2018b).

The temperature dipole in cosmic microwave background radiation caused by the motion of the Solar system barycenter with respect to the cosmic microwave background rest coordinate (e.g., Hinshaw et al., 2009) of 370 km/s induces a maximum secular parallax of 78 μas/yr/Mpc. Proper motions measured with accuracy 1 μas/yr will allow to detect a secular parallax within 78 Mpc. To date, there are 88 RFC objects within that distance. Although peculiar velocities of individual objects will cause a bias and variance in attempt to measure the secular parallax that signal has a distinctive correlation structure with quadrupolar, octupolar, and higher-order angular structure due to correlations in the peculiar velocity field. Hall (2019) explores the measurability of the secular parallax in detail.

In order to make these cosmology tests, it is crucial to provide a long time series of VLBI astrometric observations, get high fidelity images, and trace variability of the core-shift.

4 Contribution of the EVN

All scientific topics addressed above should benefit from future dedicated VLBI absolute astrometry programs. There are three areas of improvement: (i) position accuracy in the southern sky, which is typically degraded by a factor of 2 compared to that in the northern sky since the VLBI networks used for absolute astrometry, predominately VLBA, is elongated along the longitude; (ii) the lower sky density at flux densities below 120 mJy at 8 GHz (Petrov et al., 2019b) and lower position accuracy at declinations below $-45°$ due to the sparseness of VLBI radio telescopes in the southern hemisphere; (iii) getting high fidelity images for correcting astrometry data analysis for sources structure. By providing long meridianal baselines, from Europe to the Hartebeesthoek antenna in South Africa and in the future to antennas of the developing African VLBI Network (Gaylard et al., 2011), it can help to break the asymmetry in position accuracy along right ascension and declination. Incorporating The mid-frequency Square Kilometre Array SKA1-MID, (Schediwy et al., 2019) as an element of the array will also largely improve its sensitivity and accuracy in declinations, hence permitting to expand considerably the astrometric catalogue.

References

Beasley A. J., Gordon D., Peck A. B., Petrov L., MacMillan D. S., Fomalont E. B., Ma C., 2002, ApJS, 141, 13

Begelman M. C., Blandford R. D., Rees M. J., 1980, Nature, 287, 307

Blandford R. D., Königl A., 1979, ApJ, 232, 34

Cohen M. H., Shaffer D. B., 1971, AJ, 76, 91

Collioud A., Charlot C., 2014, in Bourda G., Collioud A., Charlot C., eds, Proceedings of the 19th European VLBI for Geodesy and Astrometry Working Meeting. p. 19

Condon J. J., Darling J., Kovalev Y. Y., Petrov L., 2017, ApJ, 834, 184

Darling J., Truebenbach A., Paine J., 2018a, in Murphy E., ed., Astronomical Society of the Pacific Conference Series Vol. 517, Science with a Next Generation Very Large Array. p. 813 (arXiv:1807.06670)

Darling J., Truebenbach A. E., Paine J., 2018b, ApJ, 861, 113

Dehant V., Mathews P. M., 2015, Precession, Nutation and Wobble of the Earth. Cambridge University Press, doi:10.1017/CBO9781316136133

Dehant V., Laguerre R., Rekier J., Rivoldini A., Triana S. A., Trinh A., Hoolst T. V., Zhu P., 2017, Geodesy and Geodynamics, 8, 389

Deller A. T., Middelberg E., 2014, AJ, 147, 14

Deller A. T., Boyles J., Lorimer D. R., Kaspi V. M., McLaughlin M. A., Ransom S., Stairs I. H., Stovall K., 2013, ApJ, 770, 145

Deller A. T., et al., 2019, ApJ, 875, 100

Fomalont E. B., Petrov L., MacMillan D. S., Gordon D., Ma C., 2003, AJ, 126, 2562

Frouard J., Johnson M. C., Fey A., Makarov V. V., Dorland B. N., 2018, AJ, 155, 229

Gaylard M. J., et al., 2011, in Basson I., Botha A. E., eds, Proceedings of SAIP2011, the 56th Annual Conference of the South African Institute of Physics. p. 425

Gordon D., et al., 2016, AJ, 151, 154

Gwinn C. R., Eubanks T. M., Pyne T., Birkinshaw M., Matsakis D. N., 1997, ApJ, 485, 87

Hall A., 2019, MNRAS, 486, 145

Hinshaw G., et al., 2009, ApJS, 180, 225

Immer K., et al., 2011, ApJS, 194, 25

Kopeikin S. M., Makarov V. V., 2006, AJ, 131, 1471

Kovalev Y. Y., Petrov L., Fomalont E. B., Gordon D., 2007, AJ, 133, 1236

Kovalev Y. Y., Lobanov A. P., Pushkarev A. B., Zensus J. A., 2008, A&A, 483, 759

Kovalev Y. Y., Petrov L., Plavin A. V., 2017, A&A, 598, L1

Kovalevsky J., 2003, A&A, 404, 743

Kurayama T., Sasao T., Kobayashi H., 2005, ApJ, 627, L49

Kutkin A. M., Pashchenko I. N., Sokolovsky K. V., Kovalev Y. Y., Aller M. F., Aller H. D., 2019, MNRAS, 486, 430

Lindegren L., et al., 2016, A&A, 595, A4

Liu J.-C., Zhu Z., Liu N., 2018a, AJ, 156, 13

Liu J.-C., Malkin Z., Zhu Z., 2018b, MNRAS, 474, 4477

Liu N., Zhu Z., Liu J.-C., 2018c, A&A, 609, A19

Ma C., et al., 1998, AJ, 116, 516

Makarov V. V., Frouard J., Berghea C. T., Rest A., Chambers K. C., Kaiser N., Kudritzki R.-P., Magnier E. A., 2017, ApJ, 835, L30

Mathews P. M., Herring T. A., Buffett B. A., 2002, Journal of Geophysical Research: Solid Earth, 107, ETG 3

Mignard F., et al., 2016, A&A, 595, A5

Petrov L., 2011, AJ, 142, 105

Petrov L., 2012, MNRAS, 419, 1097

Petrov L., 2013, AJ, 146, 5

Petrov L., 2016, preprint, (arXiv:1610.04951)

Petrov L., Boy J.-P., 2004, Journal of Geophysical Research (Solid Earth), 109, B03405

Petrov L., Kovalev Y. Y., 2017a, MNRAS, 467, L71

Petrov L., Kovalev Y. Y., 2017b, MNRAS, 471, 3775

Petrov L., Taylor G. B., 2011, AJ, 142, 89

Petrov L., Kovalev Y. Y., Fomalont E. B., Gordon D., 2005, AJ, 129, 1163

Petrov L., Kovalev Y. Y., Fomalont E. B., Gordon D., 2006, AJ, 131, 1872

Petrov L., Kovalev Y. Y., Fomalont E. B., Gordon D., 2008, AJ, 136, 580

Petrov L., Kovalev Y. Y., Fomalont E. B., Gordon D., 2011a, AJ, 142, 35

Petrov L., Phillips C., Bertarini A., Murphy T., Sadler E. M., 2011b, MNRAS, 414, 2528

Petrov L., Kovalev Y. Y., Plavin A. V., 2019a, MNRAS, 482, 3023

Petrov L., de Witt A., Sadler E. M., Phillips C., Horiuchi S., 2019b, MNRAS, 485, 88

Plavin A. V., Kovalev Y. Y., Pushkarev A. B., Lobanov A. P., 2019a, MNRAS, 485, 1822

Plavin A. V., Kovalev Y. Y., Petrov L. Y., 2019b, ApJ, 871, 143

Porcas R. W., 2009, A&A, 505, L1

Pushkarev A. B., Hovatta T., Kovalev Y. Y., Lister M. L., Lobanov A. P., Savolainen T., Zensus J. A., 2012, A&A, 545, A113

Reid M. J., Honma M., 2014, ARA&A, 52, 339

Reid M. J., Menten K. M., Zheng X. W., Brunthaler A., Xu Y., 2009, ApJ, 705, 1548

Reid M. J., McClintock J. E., Narayan R., Gou L., Remillard R. A., Orosz J. A., 2011, ApJ, 742, 83

Reid M. J., et al., 2014, ApJ, 783, 130

Rosat S., Lambert S. B., Gattano C., Calvo M., 2017, Geophysical Journal International, 208, 211

Schediwy S. W., Gozzard D. R., Gravestock C., Stobie S., Whitaker R., Malan J. A., Boven P., Grainge K., 2019, Publ. Astron. Soc. Australia, 36, e007

Shu F., Petrov L., Jiang W., McCallum J., Yi S.-O., Takefuji K., Li J., Lovell J., 2016, preprint, (arXiv:1605.07036)

Sokolovsky K. V., Kovalev Y. Y., Pushkarev A. B., Lobanov A. P., 2011, A&A, 532, A38

Titov O., Lambert S. B., Gontier A. M., 2011, A&A, 529, A91

Xu Y., et al., 2013, ApJ, 769, 15